

AD 709556

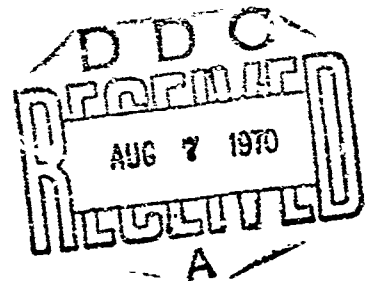
NRL Report 7111

# Fabrication and Characterization of Hot Pressed $\text{Al}_2\text{O}_3$

ROY W. RICE

*Inorganic Chemistry Branch  
Chemistry Division*

July 7, 1970



Reproduced by the  
CLEARINGHOUSE  
for Federal Scientific & Technical  
Information Springfield Va 22151

**NAVAL RESEARCH LABORATORY**  
**Washington, D.C.**

This document has been approved for public release and sale; its distribution is unlimited.

## CONTENTS

Abstract	iv
Problem Status	ii
Authorization	ii
INTRODUCTION	1
EXPERIMENTAL TECHNIQUE	1
Materials and Fabrication	1
Testing and Analysis	2
RESULTS AND DISCUSSION	2
Fabrication with 2-w/o LiF Additions	2
Fabrication Using A and B Powders Without LiF	6
Fabrication with R and BM $Al_2O_3$	10
Changes on Annealing Hot-Pressed Bodies	11
GENERAL DISCUSSION	20
Fabrication	20
Characterization	21
SUMMARY AND CONCLUSIONS	23
ACKNOWLEDGMENTS	24
REFERENCES	25

## ABSTRACT

Hot pressing of  $\text{Al}_2\text{O}_3$  with and without  $\text{LiF}$  is described, and the resultant bodies are characterized. Addition of  $\text{LiF}$  significantly enhances densification, allowing dense bodies to be obtained at about  $1100^\circ\text{C}$ , which is 200 to  $300^\circ\text{C}$  lower than without additives. However, the additives result in exaggerated grain growth even during hot pressing. Though the fluoride content is reduced, both during hot pressing and subsequent annealing, some fluoride remains which could be detrimental to some properties of bodies made with  $\text{LiF}$ . Some of the problems and defects of pressing are emphasized as an aid to improving the process. Particular attention is given to the analysis of  $\text{H}_2\text{O}$ ,  $\text{CO}_2$ , and S impurities (which are probably present as chemically bonded anions) and some of their known and possible effects on microstructure and behavior in materials made with and without additives.

## PROBLEM STATUS

This is an interim report on the problem; work is continuing.

## AUTHORIZATION

NRL Problem C05-28  
Project RR 007-02-41-5677

Manuscript submitted April 6, 1970.

## FABRICATION AND CHARACTERIZATION OF HOT PRESSED $\text{Al}_2\text{O}_3$

### INTRODUCTION

Hot pressing has improved the strength of  $\text{Al}_2\text{O}_3$  and demonstrated some of the dependence of mechanical properties on microstructure (1-3). These findings have, in turn, stimulated further use and study of the pressure-sintering process occurring during hot pressing (4-6).

This report presents the results of a study of hot-pressing  $\text{Al}_2\text{O}_3$  and the characterization and behavior of the resultant bodies. While the study was not fully completed, it supplements and expands other studies of  $\text{Al}_2\text{O}_3$  and presents new results. One of the most important results is the detection and identification of gaseous impurities\* and the demonstration of known and possible effects they can have on fabrication, microstructure, and behavior in bodies made from some of the most common sources of  $\text{Al}_2\text{O}_3$  powder used in research. This report also provides a basis for a study of the strength and fracture of dense  $\text{Al}_2\text{O}_3$  (7).

### EXPERIMENTAL TECHNIQUE

#### Materials and Fabrication

The most extensively studied materials were Linde† A and B powders (designated A and B  $\text{Al}_2\text{O}_3$ ), since they were most commonly used by other investigators (1-6). Limited tests were also made on three other alumina powders, designated as R  $\text{Al}_2\text{O}_3$ ,‡ BM  $\text{Al}_2\text{O}_3$ ,§ and C  $\text{Al}_2\text{O}_3$ .¶ The R  $\text{Al}_2\text{O}_3$ , reported to be 83% alpha alumina, was supplied as-calcined or subsequently ball-milled. The as-calcined materials were reported to have a particle-size range from 0.3 to 10 microns, averaging 1 to 2 microns, with the major impurities being 0.0023%  $\text{Fe}_2\text{O}_3$ , 0.0019%  $\text{SiO}_2$ , and 0.002%  $\text{Na}_2\text{O}$ . The ball-milled material was reported to have a somewhat finer particle size, due to the reduction of calcined agglomerates, but at the expense of increasing the  $\text{Fe}_2\text{O}_3$  and  $\text{SiO}_2$  impurities to 0.0048% and 0.0184%, respectively (9). The BM  $\text{Al}_2\text{O}_3$  had been calcined at 1000°C and had been reported to give mostly gamma  $\text{Al}_2\text{O}_3$  with some eta  $\text{Al}_2\text{O}_3$ . With particle sizes of 50 to 55 Å and purity near 99.99% except for a residual sulfur content of 0.42% (8).

Reagent-grade LiF or MgO was added to some batches by ball milling for 2 hours in isopropyl alcohol or cyclohexane in porcelain jars with high alumina grinding media. Excess fluid was decanted; then the powders were dried, screened (No. 28), and stored in sealed glass jars.

Note: Most of the data for this report was obtained while the author was in the Space Division of the Boeing Company, Seattle, Washington.

\*The term gaseous impurities refers to species such as  $\text{H}_2\text{O}$ ,  $\text{CO}_2$ , and S, which may be present as physically adsorbed or trapped gases but are more likely chemically bonded anions.

†Linde Division of Union Carbide.

‡Reynolds RC-965, Courtesy of D.V. Royce, Jr., of the Research and Development Division of Reynolds Metals Company.

§Courtesy of J.L. Henry of the Bureau of Mines Research Center, Albany, Ore. (8).

¶Alon C, product of Cabot Corporation, 125 High St., Boston, Mass.

Powders were cold-pressed in graphite dies at about 2000 psi and then vacuum hot-pressed. Some specimens containing LiF were pressed in a hot press open to the atmosphere as previously described (10,11). Most specimens were 1.5 in. in diameter and 0.1 to 0.3 in. thick (two or three were usually pressed simultaneously in a 4-in. or 6-in. die), but some 1-in.-thick cylinders were also made (one at a time). The heating rates for hot pressing were of the order of 2000°C/hr.

#### Testing and Analysis

Bars (typically 0.23 in by 0.1 in.) were cut (usually with their width being the thickness of the pressed disk), diamond ground (320 grit), and sanded (dry, through 600-grit SiC). After the above machining, many specimens were annealed (resting on edge near their ends on MgO single crystals in recrystallized  $\text{Al}_2\text{O}_3$  trays inside 99% pure MgO muffles). All initial annealing was done with a slow (2- to 3-day) heatup to 1100°C with any subsequent annealings at normal furnace rates. Silicon carbide resistance-heated furnaces and a  $\text{ZrO}_2$ -lined oxygen-natural gas furnace (used with excess oxygen) were used below and above 1650°C, respectively.

Analysis was generally by standard techniques. Densities were obtained by using Archimede's Principle (using distilled  $\text{H}_2\text{O}$ ) for dense bodies and physical dimensions for very porous samples (3.986 g/cc was used as the theoretical density (12)). Linear intercepts were taken as the grain size from photos obtained near the tensile surface of fractured bars, either on the fracture surface or by limited polishing of the surface (for some optical examination). Mass spectrometry was performed with a Bendix time-of-flight spectrometer using about 1-g samples with a tungsten crucible for a Knudsen cell (10,13).

## RESULTS AND DISCUSSION

### Fabrication with 2-w/o LiF Additions

**Densification and Forming** — Results of early pressing trials without vacuum and later ones with vacuum for various powders showed (Fig. 1) that there was no substantial difference between the densification of the A and B powders but that C was clearly more difficult to densify. The data indicate that additions of MgO may reduce the rate of densification some, that vacuum hot pressing makes no obvious difference, and that higher pressure may be somewhat beneficial. Other tests indicated that longer times increased densities (e.g., both the A and B powders with 2-w/o LiF gave about 99% or more of the theoretical density when pressed at 1095°C\* with 5000 psi for 30 minutes).

A trial back extrusion (Fig. 2) showed that  $\text{Al}_2\text{O}_3$  was somewhat less plastic than CaO (10) or MgO (11) with LiF but shows definite feasibility of some hot formability with LiF.

Comparative sintering trials (Table 1) show that LiF does enhance the sintering of  $\text{Al}_2\text{O}_3$  but not nearly as much as it does for MgO (e.g., MgO was cold-pressed to 41% of the theoretical density and sintered to 75% and 94% of the theoretical density without and with 2-w/o LiF, respectively) (13).

\*Specific operating temperatures were measured in degrees Fahrenheit but are converted here to the nearest 5°C.

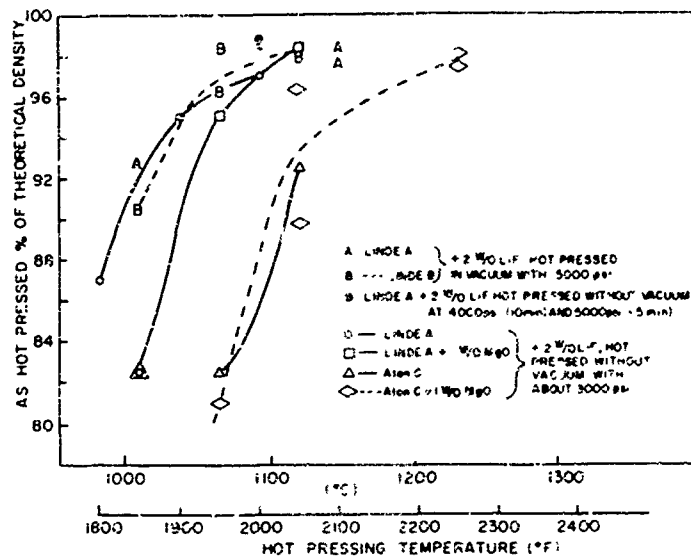
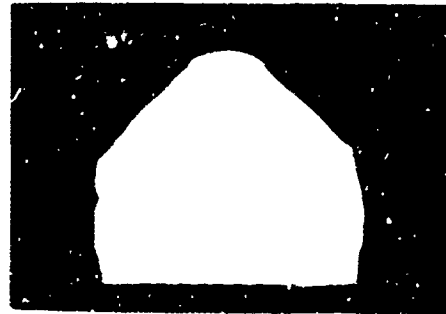


Fig. 1 - Hot pressing  $\text{Al}_2\text{O}_3$  with LiF. All specimens were held at pressing temperature for 15 minutes.

Fig. 2 - Cross section of  $\text{Al}_2\text{O}_3$  + LiF extrusion. The body of  $\text{Al}_2\text{O}_3$  + 0.5% MgO was hot pressed with 2 w/o LiF at 1850°F (1010°C) with 3300 psi for 5 minutes and then cooled. A hollow graphite ram with a conical entrance replaced the solid top ram for a back-extrusion trial at 2000°F (1095°C) with a pressure of approximately 4500 psi. In 15 minutes, the flat disk filled the conical cavity and just started to extrude into the approximately 0.4% diameter cavity. Note the faint lines indicating fairly laminar flow. Note also the black core.



15"

Table 1  
Sintering  $\text{Al}_2\text{O}_3$  In Air

Material	Cold Pressed* at 1000 psi	Density (g/cc)	% Theo- retical Density	Fired				Final Thickness (in.)
				At 1100°C		At 1300°C		
				Density (g/cc)	% Theo. Density	Density (g/cc)	% Theo. Density	
A	4	0.98	25	1.05	26	1.09	27	0.32
A	8†	1.20	30	1.21	30	1.39	35	0.42
B	4‡	0.55	14	0.62	16	1.29	32	0.45
B	8†	0.83	21	0.85	21	1.34	34	0.36
A + 2w/o LiF	4†	1.27	32	1.49	37	1.76	44	0.41
A + 2w/o LiF	8†	1.12	28	1.74	44	1.75	44	0.30
A + 2w/o LiF	12†	1.10	28	1.20	30	1.54	39	0.39
B + 2w/o LiF	4	0.54	14	1.03	26	1.15	29	0.35
B + 2w/o LiF	4	0.64	16	1.18	30	1.18	30	0.42
B + 2w/o LiF	(slugged 4)§	0.87	22	1.35	34	1.38	35	0.30
	8 (slugged 4)							

\*Approximately 8 grams in a 1.125-in.-diam die gave die fills of about 1.5 in. for the A powder and about 2.5 in. for the B powder.

†Some limited lamination.

‡Extensive lamination.

§Powder pressed at 4000 psi, broken and repressed, as shown.

**Characterization of Hot-Pressed Bodies** — Specimens from the A and B powders had a dull, opaque, white appearance up to about 95% of the theoretical density. Beyond this limit, specimens became progressively glossier (when ground or sanded), showed some surface translucency, and generally began to show some gray-to-blue tint and darker gray-to-black cores (Figs. 2 and 3). Such cores were more common in the specimens of B  $\text{Al}_2\text{O}_3$ , near the bottom of the specimens (i.e., in a slightly cooler or slower heating area of the specimen) and in thicker bodies. Specimens from the C powder were a dull, opaque white at lower densities and a light dull gray at higher densities (possibly somewhat grayer with MgO additions).

Sample analysis using a light element detector on an electron probe is shown in Table 2, indicating that while much of the additive is lost during hot pressing, a substantial portion of at least the fluorine is retained. The lower relative increase in density in smaller or more porous samples on raising the sintering temperature from 1100 to 1300°C (Table 1) indicates a greater loss of the fluoride with decreasing size and density as expected and observed for MgO (13,14) and CaO (10,14). The probe showed no obvious significant inhomogeneities in the fluorine distribution, but because of the fine grain size, this does not mean that the fluorine was not at grain boundaries where it is observed in CaO (9) and MgO (10).

The microstructure of specimens from both the A and B powders showed a duplex grain structure most commonly with large tabular (Fig. 4a) and sometimes more equiaxed grains (Fig. 4b). In some cases, there was some possible local alignment of the large tabular grains. Limited trials using up to 1-w/o MgO additions showed no sign of suppressing this inhomogeneous exaggerated grain growth.

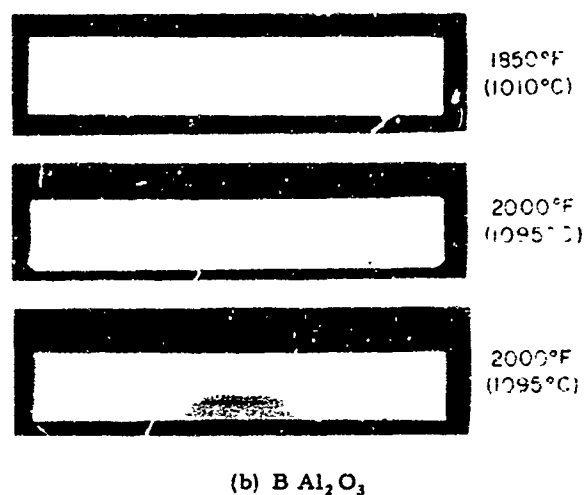
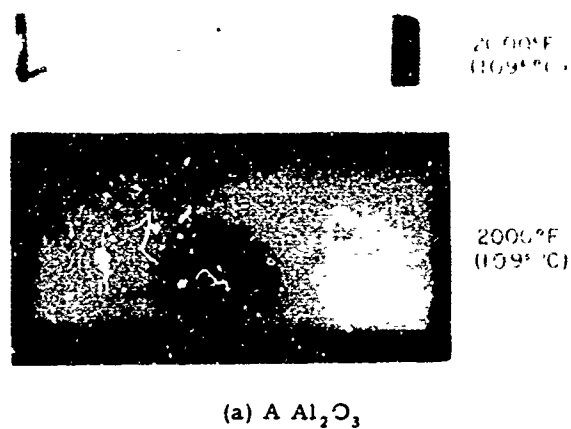


Fig. 3 - Cross sections of  $\text{Al}_2\text{O}_3$  hot pressed with LiF. All specimens (approximately 1.5-in. diameter cross section) were hot-pressed at about 5000 psi for 15 minutes (except the last, which was 30 minutes) at temperatures shown at the right. Note tendency for black core to be nearer the bottom (cooler) side.

Table 2  
Fluorine Analysis by Electron Probe

Powder Sample	Temperature at which Hot-Pressed (°F)	Approximate F Content (a/o)*	
		After Hot Pressing	Subsequent Annealing to 2150°F (1175°C)
A	1950	0.59	0.18
B	2050	0.48	0.20

\*The original level of fluorine addition was 1.43 a/o.



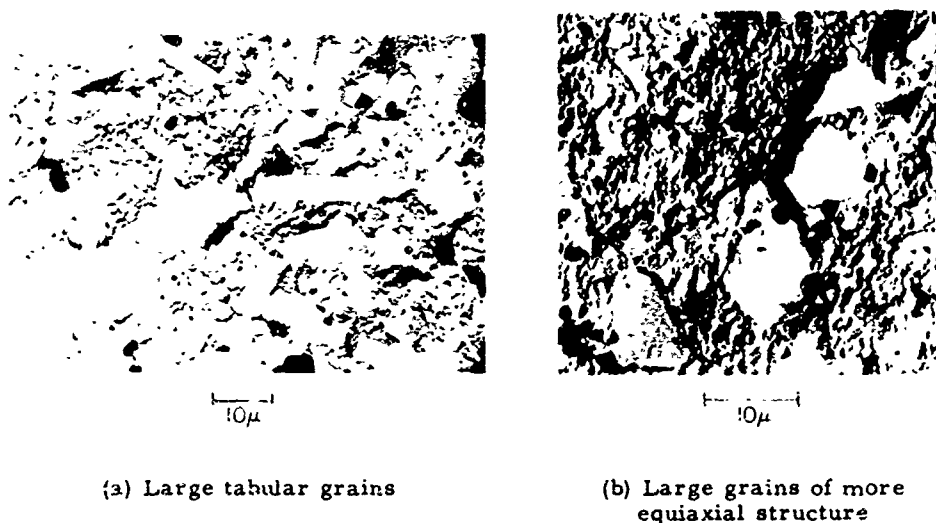


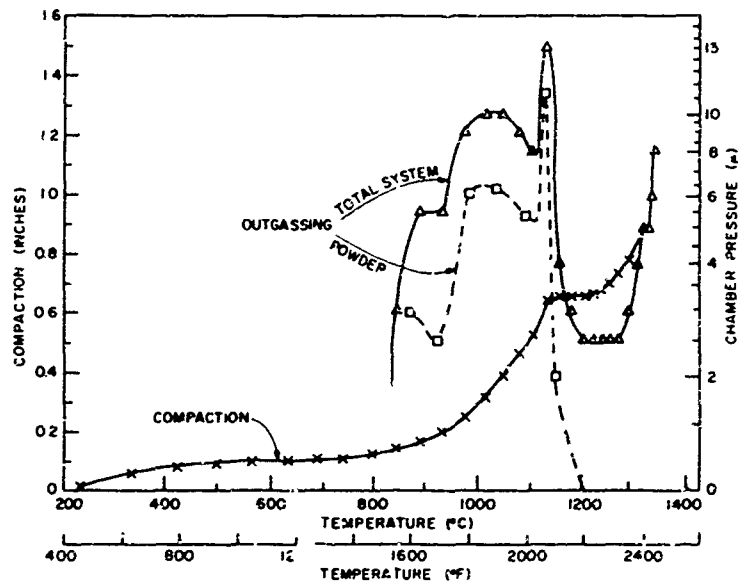
Fig. 4 - Examples of exaggerated grain growth in  $\text{Al}_2\text{O}_3 + \text{LiF}$  during hot pressing. Both occurred in specimens with and without vacuum during hot pressing.

#### Fabrication Using A and B Powders Without LiF

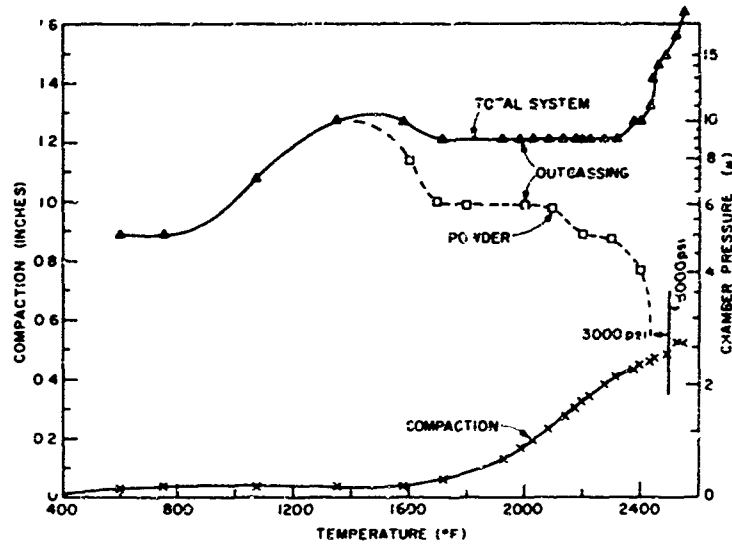
**Densification** — All hot pressing without additions of LiF was done in vacuum. Powder outgassing varied considerably during heating. However, there were fairly consistent differences between the shapes of the outgassing curves for different raw materials as shown by representative examples in Fig. 5. The rate of compaction was generally highest during the latter part of the outgassing (Fig. 5).

Because of the above outgassing and compaction behavior, pressure was generally not applied until a temperature of about  $1200^\circ\text{C}$  was reached. However, if pressure was not applied by the time a temperature of  $1300$  to  $1400^\circ\text{C}$  was reached, the powder (especially B) would begin to shrink away from the die walls (Fig. 7). An under-sized and lower density specimen normally resulted if substantial shrinkage occurred before pressure (e.g., 5000 psi) was applied.

A series of specimens was hot-pressed (mostly from the same batch of a given powder) for two to five different times under a given pressure for given temperatures; then a density-temperature-time plot was made for that pressure. Both A and B  $\text{Al}_2\text{O}_3$  showed quite limited scatter for achieving porosities of a few percent or less, with scatter tending to increase with increasing porosity (especially for B  $\text{Al}_2\text{O}_3$ ). Cuts from these curves are shown, with supplemental data (some from other investigators), in Fig. 6, which also indicates the range of parameters investigated. Data from other lots generally agreed fairly well with the data of Fig. 6, but more scatter occurred with some batches (i.e., different packages, especially of different lots). The data for cylinders about 1 in. long appear to fall within the scatter expected from different batches and different initiation of ram pressure. Dense, fine-grain bodies, having the greatest strength ( $100,000 \pm 10,000$  psi) at room temperature, were obtained by hot pressing in the range of  $1250$  to  $1350^\circ\text{C}$ , with a pressure of 7500 psi applied  $0^\circ$  to  $50^\circ\text{C}$  before the maximum temperature and held for 90 to 60 minutes. Increasing the pressure to 10,000 psi to lower the temperatures or times made no noticeable reduction in the grain size and gave the same or lower strengths (see Ref. 7 for strength data). Full pressure was reached as the hot-pressing temperature was reached and then released in a minute or less at the end of the holding-at temperature.



(a)  $\Delta \text{Al}_2\text{O}_3$ . Compaction is under 3000 psi for most of the test; then 5000 psi, as indicated.



(b) B  $\text{Al}_2\text{O}_3$ . Compaction is under 3000 psi.

Fig. 5 - Vacuum outgassing and compaction of the A and B powders. This outgassing is after pumping overnight. Both samples were about 30 grams.

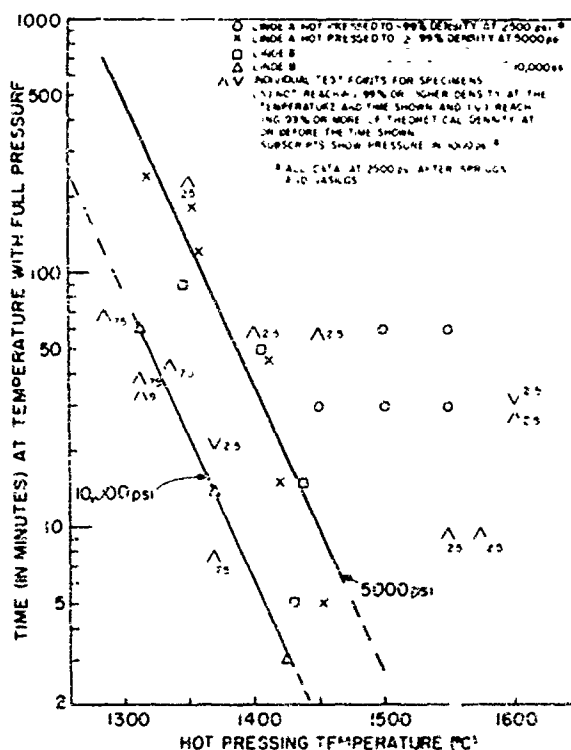


Fig. 6 - Time versus temperature to achieve 1% or less porosity in hot-pressed  $\text{Al}_2\text{O}_3$

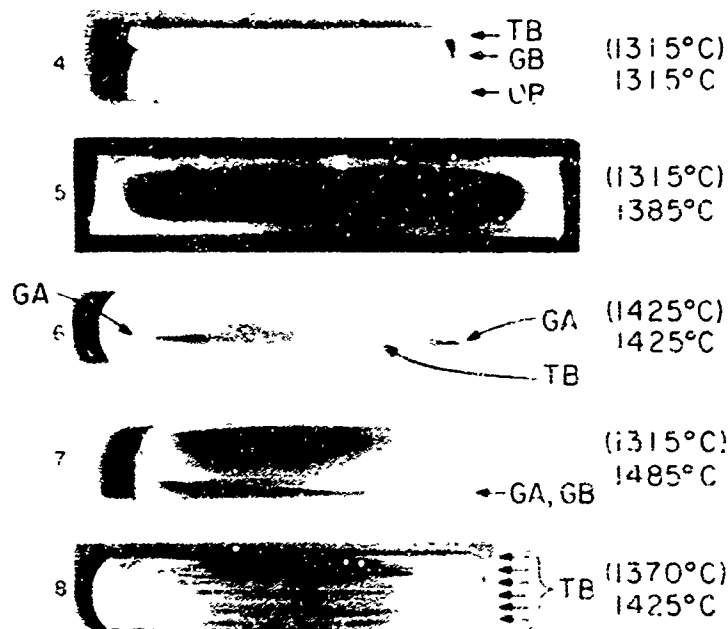
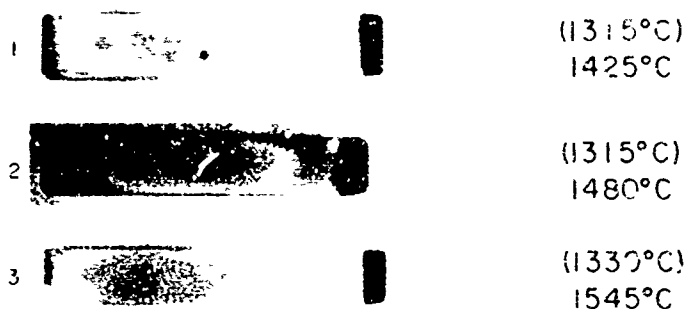
One set of specimens fabricated from A  $\text{Al}_2\text{O}_3$  at 1485°C with 5000 psi (applied at 1315°C) for 90 minutes was translucent (referred to as A'). The top specimen was completely translucent, but the lower specimen in the die had an opaque, gray, lenticular area about one-half the diameter of the disk approximately centered in the disk. Otherwise, there were no obvious inhomogeneities in the densification of A  $\text{Al}_2\text{O}_3$ .

Much of the B  $\text{Al}_2\text{O}_3$  also gave no obvious sign of inhomogeneous densification. A few specimens fabricated at marginal conditions (and usually near the bottom of the die where there was some thermal gradient) showed a fairly uniform transition from translucency to opacity similar to Sample 4 of Fig. 7. However, inhomogeneities in densification, of which Samples 6 and 8 in Fig. 7 represent a fair range, were not infrequent with B  $\text{Al}_2\text{O}_3$ .

After hot pressing either A or B powders, both the vacuum chamber and many specimens had a distinct sulfur smell, which often became quite strong with higher temperature pressings. After some of the higher temperature pressing, a yellow-to-brown dust was deposited on the upper rams, which decreased in quantity with distance from the die.

Limited trials of  $\text{Al}_2\text{O}_3$  with MgO additions indicated no significant differences in fabrication due to 1% or less MgO additions.

(a)  $\text{Al}_2\text{O}_3$  specimens  
pressed with 5000 psi  
for 15 minutes



(b)  $\text{Al}_2\text{O}_3$  specimens



Fig. 7 - Cross sections of  $\text{Al}_2\text{O}_3$  vacuum hot-pressed without additives. Figures at the right refer to the temperatures of starting pressure and hot pressing. Cross sections are all 1.2 to 1.5 in. in diameter. Note rounding of edges due to shrinkage from the die. GA and GB refer to green areas and green bands, and OB and TB refer to opaque and translucent bands. Other coloration was as seen in the photos. Samples 4 through 6 were pressed with 10,000 psi for 90, 60, and 5 minutes, respectively. Sample 4 was nearer the bottom of the die. Samples 7 and 8 were pressed with 5000 psi for 15 minutes. Note the black areas in Samples 5 and 7 and many fine bands in Sample 8 that had a gray-orange appearance in transmission. BM  $\text{Al}_2\text{O}_3$  was hot-pressed with 5000 psi for 30 minutes. Note that the bands are made up of light green translucent patches and irregular edges due to shrinking away from the die.

**Body Characterization** — Many of the dense specimens had dense, glossy, black areas which were often lenticular in shape but were not infrequently irregular in  $B Al_2O_3$  (Fig. 7). The largest, glossiest, and blackest cores (e.g., Sample 5 of Fig. 7) occurred with dense  $B Al_2O_3$  fabricated at lower temperatures with the greatest (10,000 psi) pressure. Black or gray cores were also frequent in  $A Al_2O_3$  bodies, usually less pronounced in coloring, and often with some faint circumferential banding (also sometimes seen in  $B Al_2O_3$ ), as shown in Fig. 7.

In addition to these larger colored areas, many specimens had small gray-to-black specks. These were observed most commonly by grinding a surface parallel to the top or bottom of the pressed disk. They were visible to the unaided eye in sizes of less than 0.01 in. to over 0.05 in. Their distribution was not homogeneous, varied from specimen to specimen, and showed no radial pattern. Most appeared to be relatively thin and somewhat irregular in shape. A sampling of 12 disks showed that at least 9 contained such specks with the number varying from a few to a hundred or more (e.g., in a  $B Al_2O_3$  sample).

Grain sizes of the most dense A and  $B Al_2O_3$  hot pressed near the parameters shown in Fig. 6 usually averaged about 1 micron; however, threefold variations over limited dimensions were not uncommon (Fig. 13). Generally, bodies of the finest (1-micron or less) grain size were the least reproducible. In addition to approximate random variations, there were sometimes bands of finer grains (Fig. 8), generally oriented parallel to the pressing surfaces. Specimens pressed at higher temperatures and longer times had larger grain sizes (e.g., the translucent A disks mentioned earlier had grain sizes of 15 to 25 microns). Hot-pressed grains, especially those less than 10 microns, were generally equiaxed. Almost all porosity was at the grain boundaries in hot-pressed bodies.

X-ray analysis of  $B Al_2O_3$  bodies showed that no detectable gamma phase was left after hot pressing. A few very weak, unidentified (and not always consistent) lines were found in some bodies of both A and  $B Al_2O_3$ .

#### Fabrication with R and BM $Al_2O_3$

Trial fabrication parameters and results for R and BM  $Al_2O_3$  are shown in Table 3. BM-1 and BM-3 had clearly shrunk away from the die before pressure was applied and were not pressed back to full contact (e.g., Sample 9 of Fig. 7). Some fine cracking near the edge indicated that BM-2 had also shrunk away from the die some but was expanded back in contact with it, showing that this fine powder begins rapid densification at lower temperatures. After hot pressing R  $Al_2O_3$ , some sulfur smell was left in the vacuum chamber. During the pressing of the BM  $Al_2O_3$ , even the vacuum-pump exhaust had a strong sulfur smell.

The resultant R  $Al_2O_3$  bodies were an even opaque white, as was BM-2 (Table 2). However, the other two BM  $Al_2O_3$  disks had gray and green translucent bands, usually consisting of small, lenticular areas. In BM-3, these were mostly in the top of the disk in a central area about 0.5 in. in diameter, while in BM-1, they were mostly in two bands (Fig. 7).

Grain sizes of the BM bodies average 1 to 1.5 microns. However, bands of finer grains parallel with the pressing (ram) surfaces were frequently observed (more so than with  $B Al_2O_3$ ).

Fig. 8 - Fine grain bands found in some hot-pressed  $\text{Al}_2\text{O}_3$  bodies. Some were in A  $\text{Al}_2\text{O}_3$  bodies, more were in B  $\text{Al}_2\text{O}_3$ , and BM  $\text{Al}_2\text{O}_3$  appeared to have somewhat more than B  $\text{Al}_2\text{O}_3$ .

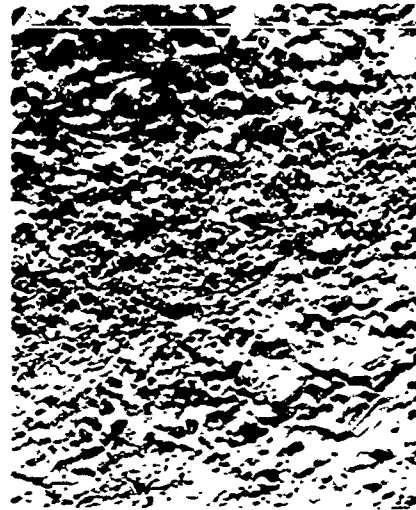


Table 3  
Vacuum Hot Pressing of R and BM  $\text{Al}_2\text{O}_3$

Specimen*	Temp. at Which Pressure Was Started	Maximum Ram Pressure (1000 psi)	Temperature Held At	Time Held For (min)	Resulting % of Theoretical Density
R-1	2400°F (1315°C)	7.5	2700°F (1480°C)	15	94
R-2	2400°F (1315°C)	10.0	2400°F (1315°C)	60	93
R-3					92
R-4	2400°F (1315°C)	10.0	2600°F (1425°C)	60	97
R-5	2400°F (1315°C)	10.0	2650°F (1455°C)	60	97
BM-1†	2400°F (1315°C)	5.0	2550°F (1400°C)	30	95
BM-2	2200°F (1205°C)	7.5	2400°F (1315°C)	60	85
BM-3†	2350°F (1289°C)	7.5	2500°F (1370°C)	60	93

\*All specimens were 1.5 in. in diameter. R-1 was 1 in. thick. All others were about 0.3 in. thick. R-1 was not ball milled; all other R specimens were of ball-milled material.

†Specimens shrunk away from the die before pressure was applied (see Fig. 7).

#### Changes on Annealing Hot-Pressed Bodies

**Appearance** — Black, gray, and green colors disappeared progressively inward from the fired surfaces with increased annealing in air above 1200 to 1300°C. Temperatures of at least 1600°C were required to eliminate the last traces of color from the center of some bars which were about 0.1 in. thick and cut from some of the darker specimens. The resultant appearance was usually white and often slightly translucent (usually not observed unless annealing was above about 1600°C). The exception was R  $\text{Al}_2\text{O}_3$ ; these samples had a yellow tint (and often some slight translucency) after air annealing at 1650°C and higher.

Many previously opaque specimens became slightly translucent on annealing, but previously translucent sections or pieces often decreased some in translucency (e.g., the two translucent A  $\text{Al}_2\text{O}_3$  bodies).



Fig. 9 - Bloating in a  $B Al_2O_3$  body (that had a black core) during annealing at  $1815^\circ C$ . Note the original pressing direction (indicated by arrow) showing that this is not a laminar defect.

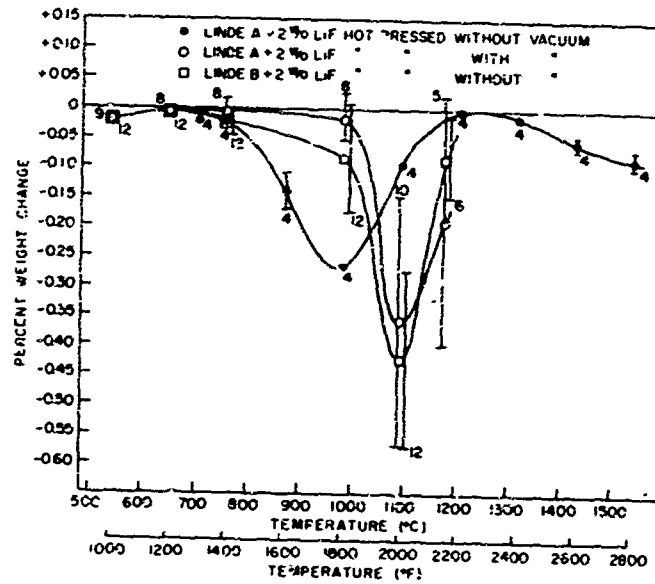


Fig. 10 - Annealing weight change of Linde  $Al_2O_3$  hot pressed with 2-w/c LiF. Bars from hot-pressed disks were heated, annealed for 1 hour in air, cooled, and weighed for each temperature point. Points represent averages, vertical bars (or symbol height) represent the standard deviation, and sub-(or super)scripts represent the number of bars. All bars from the specimens hot pressed without vacuum are from one hot-pressed disk, 0.1 in. thick; the other tests generally represent two bars from each of several disks about 0.25 in. thick.

In a few of the dense B  $\text{Al}_2\text{O}_3$  bodies with glossy black cores, bloating or blistering was observed on annealing above  $1700^\circ\text{C}$  (14) (Fig. 9).

**Density and Weight** — The density of A  $\text{Al}_2\text{O}_3$  bodies, hot-pressed with 2-w/o LiF (with or without MgO additions) without vacuum, was checked at various annealing temperatures. Densities usually decreased to a minimum on annealing at about  $1300^\circ\text{C}$ . Specimens that were 95 to 100% dense as hot pressed decreased the most (4 to 7%), but specimens 80 to 90% dense decreased some (2 to 5%). Further annealing to  $1500^\circ\text{C}$  or more raised densities to their original levels or higher (especially for less dense specimens).

Weight changes with annealing temperature are shown for some specimens hot pressed without vacuum, as well as some hot pressed in vacuum, in Fig. 10.

Specimens hot pressed without additives also changed their weight on subsequent annealing as shown in Fig. 11. A specimen of BM  $\text{Al}_2\text{O}_3$  lost 0.1 to 0.2% of its weight during vacuum heating to about  $1800^\circ\text{C}$  for mass spectroscopic analysis (see below).

**Additives and Impurities** — Table 2 shows that annealing reduces the residual fluorine content of bodies made with LiF but that measurable amounts remain. This loss of additive is supported by the greater weight losses of specimens made with LiF (Fig. 10) than without (Fig. 11). However, the losses shown in Fig. 10 are greater than the loss of LiF, showing that other material is also lost. This was corroborated by mass spectrometry (of A  $\text{Al}_2\text{O}_3$  + LiF bodies), which showed outgassing to be due to  $\text{H}_2\text{O}$  and  $\text{CO}_2$  evolution as maximums of about  $400^\circ$  and  $1200^\circ\text{C}$ , respectively, were reached.

These same gases were evolved from specimens hot pressed without LiF, though the quantities were generally lower and the temperatures higher (Fig. 12). Some species of mass 34 were found, which was attributed to  $\text{H}_2\text{S}$ . Mass spectrometer analysis of samples of A and B  $\text{Al}_2\text{O}_3$  powder showed all of these same species to be present in greater quantities than in the pressed bodies. Addition of a small amount of graphite dust to the powder increased the amount of  $\text{H}_2\text{S}$  released. Since these analyses by the author, Sellers and Niesse (15) have further analyzed some  $\text{Al}_2\text{O}_3$  powders for sulfur (Table 4).

A mass spectrometer analysis of a BM  $\text{Al}_2\text{O}_3$  body (BM-3 of Table 3) showed both mass 34 and 33 ( $\text{H}_2\text{S}$  and HS) coming off to at least  $600^\circ\text{C}$  and  $\text{H}_2\text{O}$  coming off strongly to at least  $1000^\circ\text{C}$ , with traces still observed at higher temperatures. Some  $\text{CO}_2$  was also evolved to about  $800^\circ\text{C}$ , while CO and C reached a maximum evolution at about  $1600^\circ\text{C}$ . While the lower temperatures of the  $\text{H}_2\text{S}$  and HS evolution (especially compared to A  $\text{Al}_2\text{O}_3$ ) may be partly due to the lower density, the marked difference in temperatures and the limited difference in density suggest that the sulfur of the BM  $\text{Al}_2\text{O}_3$  is held less tenaciously. This is probably one of the reasons that the much greater starting sulfur content does not result in a proportionally greater retained content.

The occurrence of these gases in larger quantity in the starting powder indicates that most or all of them in hot-pressed bodies are left from the original powder.  $\text{Al}_2\text{O}_3$  powders are commonly derived from sulfates, usually hydrated ammonium aluminum sulfates (e.g., A, B, and BM  $\text{Al}_2\text{O}_3$ ). Hot pressing in graphite probably reduces the sulfate to the sulfide which reacts with  $\text{H}_2\text{O}$  to form  $\text{H}_2\text{S}$  (16). The greater release of  $\text{H}_2\text{S}$  from  $\text{Al}_2\text{O}_3$  powder with graphite powder supports this.  $\text{H}_2\text{O}$  can come from residual water of crystallization or from the atmosphere, which is probably one of the sources of the  $\text{CO}_2$  (17), though some  $\text{CO}_2$  might come from reaction with graphite dies.



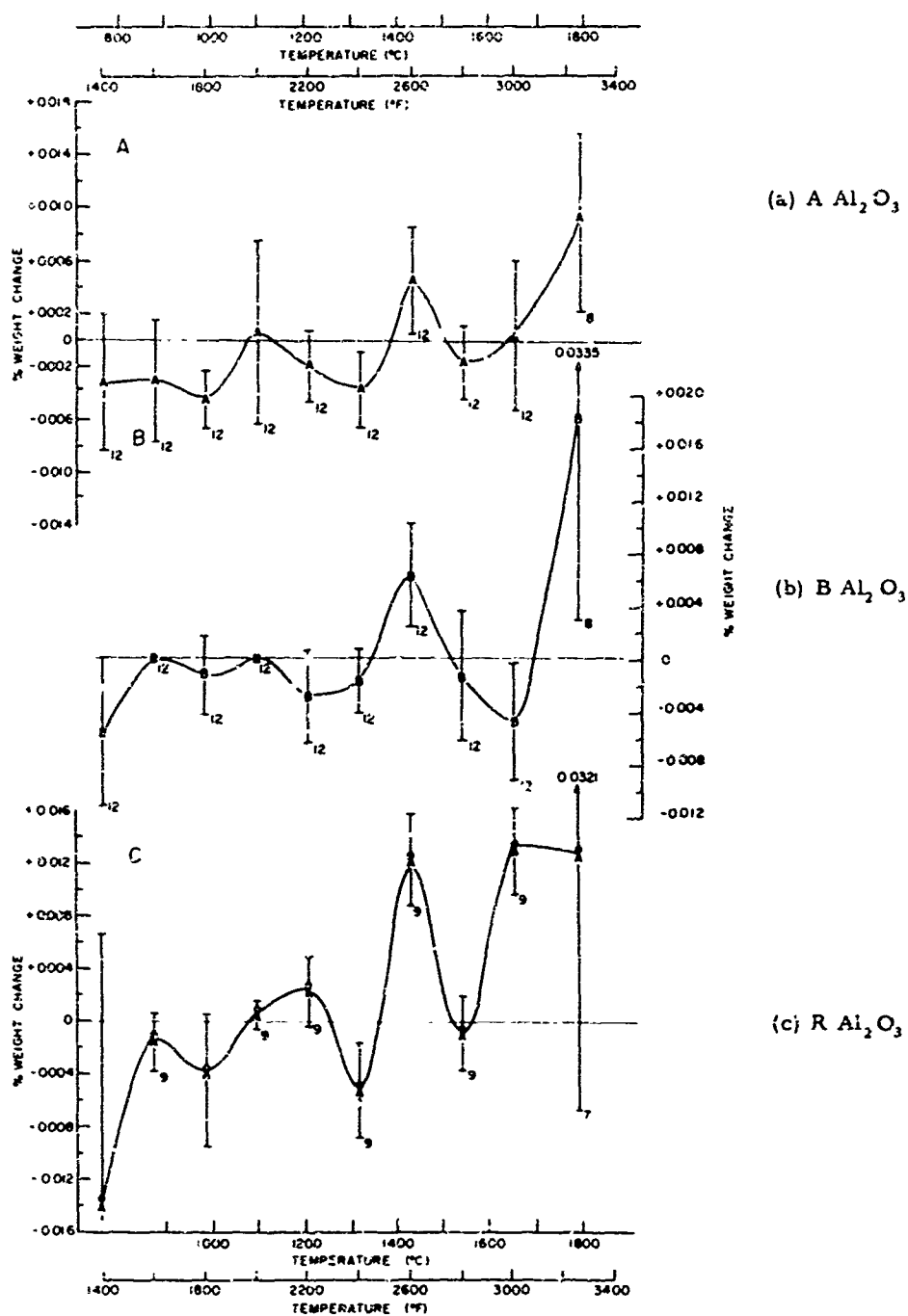


Fig. 11 - Annealing weight changes of  $\text{Al}_2\text{O}_3$  vacuum hot pressed without additives. Bars cut from hot-pressed disks were annealed in air at each temperature for 1 hour, cooled, and weighed before firing again. Each point represents the average change of weight after firing from its previous weight; vertical bars show one standard deviation, and subscripts the number of bars. Less variation occurred with bars from the same pressing.

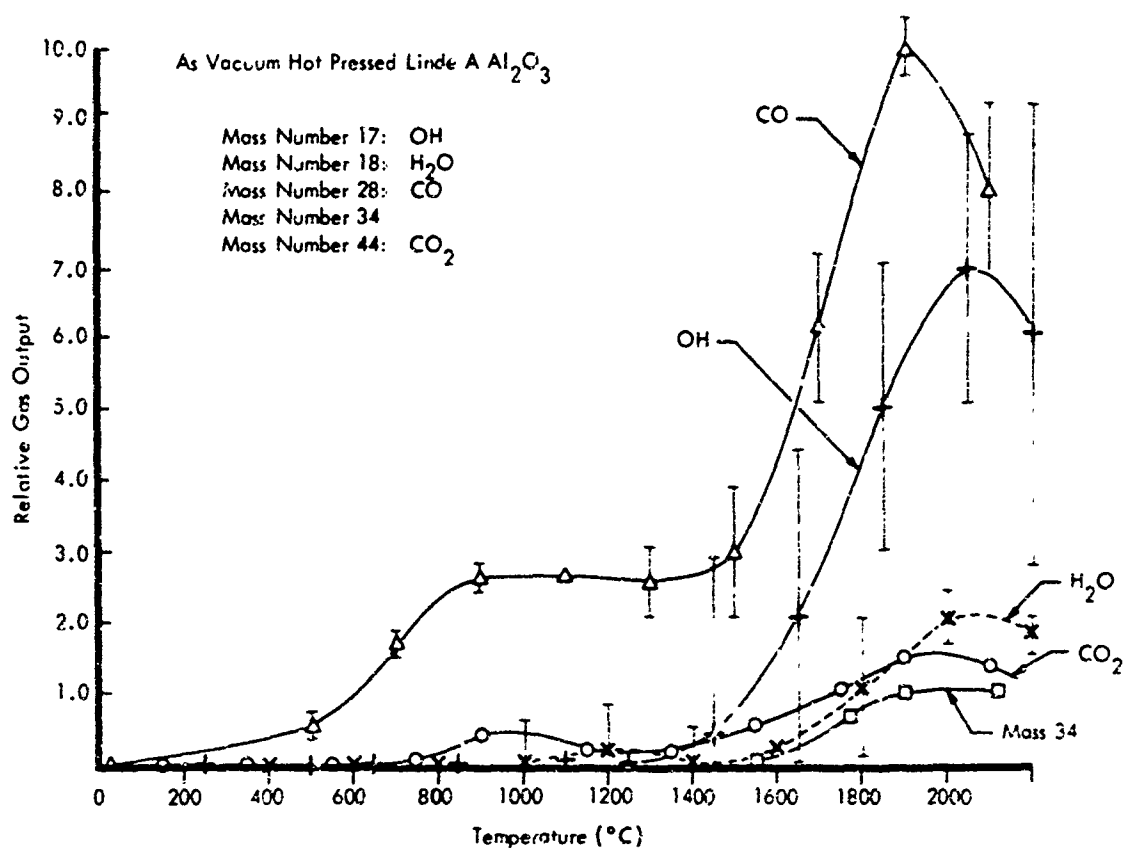


Fig. 12 - Mass spectrometer data for hot-pressed Linde A  $\text{Al}_2\text{O}_3$ . Net outgassing (from Knudsen cell), background subtracted (vertical bars represent variation in background).

Table 4  
Surface Area and Sulfur Analysis Results  
on Alumina Powders

Powder	Surface Area ( $\text{m}^2/\text{g}$ )	Sulfur Content (w/o)
Linde A Lot 1226	16.62*	0.02*
Linde A Lot 1354	16.60, 17.02*	0.02*
Meller Lot 16873-43	16.30*	0.02*
Linde "B" (0.06 $\mu$ ) Lot 1136	79.8*	0.05, 0.06*
Meller (0.05 $\mu$ ) Lot 16874-44	93.2, 95.8*	0.54, 0.56*
BM $\text{Al}_2\text{O}_3$ (1000 $^{\circ}\text{C}$ calcine)		0.42†

\*Courtesy of Dr. William Rhodes, AVCO Corp., Lowell, Mass. (13).

†See Ref. 8.

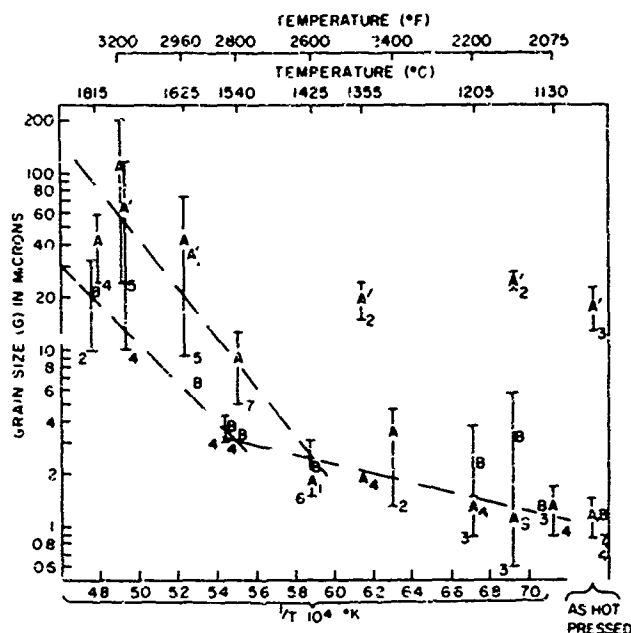
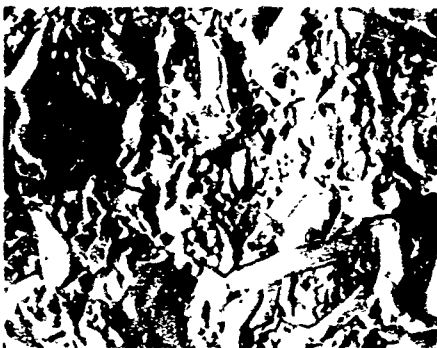
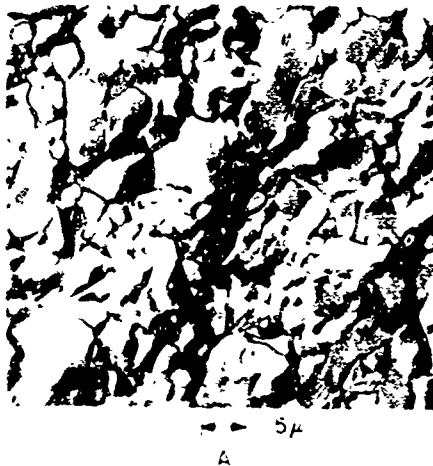


Fig. 13 - Grain growth in annealed, hot-pressed  $\text{Al}_2\text{O}_3$ . Specimens of A and B  $\text{Al}_2\text{O}_3$  were hot-pressed without additives and then annealed in air for 1 hour. Vertical bars represent the standard deviation, and subscripts represent the number of specimens (where no bar is shown for more than one specimen, deviation is smaller than the symbol). A and B for specimens hot-pressed per curves of Fig. 6, A' specimens pressed for longer times (at the higher temperatures). A single A' value of 29 microns at 4.79 is not shown due to crowding.

**Microstructure** — Grain growth of A and B  $\text{Al}_2\text{O}_3$  bodies is shown in Fig. 13. The translucent A specimens pressed for longer times at higher temperatures than shown in Fig. 6, which had some limited nonequiaxial grain structure as hot pressed, showed some limited increase of this structure on annealing. The remainder of the specimens fabricated by the curves of Fig. 6 showed very distinct exaggerated grain growth on annealing (Fig. 14). This growth often occurred inhomogeneously (e.g., in patches, especially at temperatures below 1600 to 1700°C) and seemed to be somewhat more prevalent near the surface. It was most commonly observed to have begun in dense B  $\text{Al}_2\text{O}_3$  bodies about 1400 to 1450°C and about 1500 to 1550°C in dense A  $\text{Al}_2\text{O}_3$  bodies, though there could be considerable variation (e.g., Fig. 14). The most extreme cases of this grain growth were observed in a few dense B  $\text{Al}_2\text{O}_3$  bodies with dense, black, glossy cores (Fig. 15), with extremely large grains occurring in the core area.

Surface scratches left from sanding dense A and R  $\text{Al}_2\text{O}_3$  bodies were slower in annealing. Remnants of scratches were still readily observed microscopically on the surface of some of these bodies even after annealing at 1800°C or more, though substantial annealing (e.g., rounding) was often observed by 1500 to 1600°C (Fig. 16). B  $\text{Al}_2\text{O}_3$  bodies showed easier annealing of scratches, e.g., substantial annealing by 1400°C, but temperatures of 1600°C were often required for fairly complete annealing. Such easier annealing of scratches could result from the greater quantities of gaseous impurities in these bodies leading to enhanced surface diffusion.

(a) A fairly moderate case in a  $B Al_2O_3$  body annealed at 2800°F (1540°C)



(b) A more extreme case in another specimen from the same disk annealed at 2600°F (1425°C)

Fig. 14 - Exaggerated grain growth in annealed bodies of dense hot-pressed  $Al_2O_3$

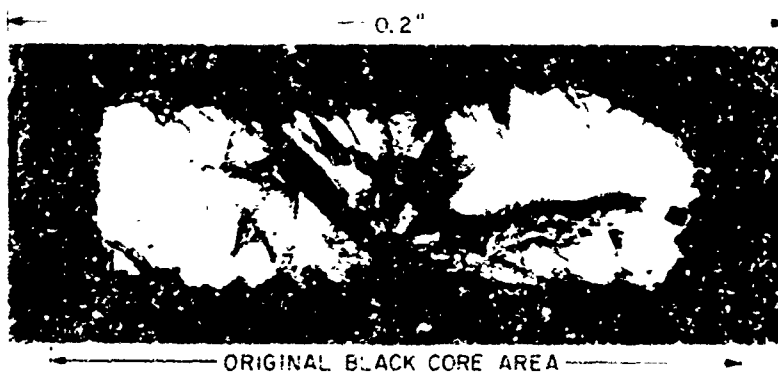
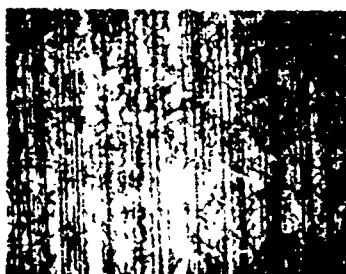


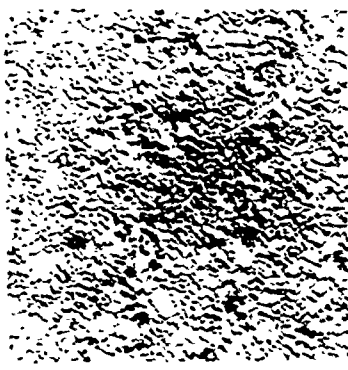
Fig. 15 - Large grains in the core area of a  $B Al_2O_3$  body (specimen fracture surface). The specimen (from the same disk as the specimen of Fig. 10) was annealed at 3300°F (1815°C). Note that much of the region previously covered by a black core (Sample 5 of Fig. 7) is now approximately 3 grains which are in the order of 1000 times the surrounding grains. These large grains contained some porosity.



(a) Optical photo of a specimen after 3250°F (1790°C) anneal



(b) Optical photo of another specimen after 2800°F (1540°C) anneal



(c) Electron micrograph of same specimen as in (b)

Fig. 16 - Microscopic observation of scratches from 600-grit sanding of dense  $\text{Al}_2\text{O}_3$  after annealing

Besides the obvious changes of porosity with observed density changes, there were two trends in porosity. The first trend was for larger pores to often appear at the grain boundaries (Fig. 17), especially in some dense bodies made without additives. The number and size of these pores often tended to increase with increasing annealing temperature, at least for temperatures of approximately 1500°C or more. At the higher temperatures (e.g., over 1700°C), such grain boundary pores often began to merge, sometimes forming channels. In the extreme (e.g., in some areas of the translucent A<sup>+</sup> specimens), a large section of a grain boundary, or even an area of several grains, would apparently become one continuous pore. However, the occurrence of such porosity was highly non-uniform, with some areas of some specimens developing a substantial number of pores, and others, few or none. Most of the resultant porosity was either not substantial or extensive enough to make obvious changes in densities. Some of these larger pores may have formed by the consolidation of smaller pores, sometimes with a net reduction of porosity, as indicated by cases of increasing translucency. However, the variations, as well as substantial cases of decreasing translucency and some definite increase in porosity, indicate that much of this porosity was due to losses of gaseous impurities. The inhomogeneity of the resulting porosity therefore reflects in part the inhomogeneity of such impurities.

The second trend in porosity was for some pores, especially finer ones, to be trapped inside of growing grains (Fig. 17). Thus, there was clearly a trend from much (usually

(a) Fracture surface. Note the pores and channels on the grain boundary surface in the top portion. Terraces are apparently not fracture marks but probably contouring due to surface diffusion where the grain boundary apparently parted during annealing. Note the finer ingrain porosity and its effect on transgranular fracture in the lower portion.



(b) Joined pores, containing one or more small dots (protrusions into pore) in most pores

Fig. 17 - Porosity in annealed dense  $\text{Al}_2\text{O}_3$  bodies

most) of the porosity being at grain boundaries in the finest grain specimens to much (sometimes most) of the porosity being within grains of large grain bodies. The latter was somewhat more frequent in annealing specimens starting with fine grain size and fine porosity (e.g., specimens not pressed to quite full density). This also occurred in annealing specimens made with LiF, especially at higher temperatures. Such trapping of porosity also occurred to some extent as a result of grain growth during hot pressing. The extreme exaggerated grains noted above in B  $\text{Al}_2\text{O}_3$  also had many trapped pores.

Spriggs et al (2) and Passmore et al (3) noted that their most dense  $\text{Al}_2\text{O}_3$  specimens increased in porosity by 1 to 3% on annealing. This must clearly be due to gaseous impurities rather than anisotropic grain growth which they suggested (2). The greater amount of porosity generated in their specimens is attributed to the lack of both vacuum hot pressing and a very slow initial annealing cycle after hot pressing.

## GENERAL DISCUSSION

### Fabrication

Without LiF — Application of Mangsen et al (18) parameters for the Mackerzie-Shuttleworth (19) equation for the densification of A  $\text{Al}_2\text{O}_3$  to 99% of theoretical density predicts densification times of 50 to several hundred percent longer than shown in Fig. 6. The data of Crandall et al (20), showing near theoretical density at times in the order of 10 minutes for temperatures over 1500°C, are also substantially longer than in this work; however, their lower pressure (2000 psi) and larger grain-size material (12 micron) probably account for much, if not all, of this difference. Gardner et al's (21) parameters of 1500°C at 6000 psi for 4 hours for hot pressing quite translucent B  $\text{Al}_2\text{O}_3$  are clearly extreme. However, they give no indication of having attempted to minimize any of these parameters. Their grain size of 10 to 30 microns is consistent with the long pressing. Data of Spriggs and Vasilos (1) (with a heating and pressing cycle similar to the author's) at 2500 psi, are shown for comparison in Fig. 6. While their data (also on A  $\text{Al}_2\text{O}_3$ ) show wider scatter, which is probably due to the lack of vacuum hot pressing and to different lots of material, it is roughly consistent with the expected shift due to lower pressure. Their results of 99.2 to 99.3% of theoretical density at 1450°C for 30 minutes on other powders (including B  $\text{Al}_2\text{O}_3$ ) with 4000 psi show good agreement with the present data (i.e., slightly longer times for somewhat lower pressure).

Rossi and Fulrath (5), also using A  $\text{Al}_2\text{O}_3$ , observed an end-point density in as-received powders, contrary to the present observations. This was attributed to trapping gaseous impurities (they assumed  $\text{H}_2\text{O}$ ) within pores. In view of the fact that they applied their pressure at 800°C and the outgassing data of Fig. 5, such trapping of gaseous impurities is not surprising. Their low pressing temperatures (1200 and 1250°C) may also have contributed to this. They reported that treatment of the powder by immersion in isopropyl alcohol, then vacuum drying for 40 hours, removed this problem, since their densification data would then extrapolate to zero porosity. However, since there are lot-to-lot variations (as shown in this work), their treatment may have been conducted on "better-than-average" powder.

Several results, though not exactly comparable, suggest that further evaluation of their treatment is necessary. First is the tenacity of the adsorbed species, as shown by the present mass spectrometry on both powders and bodies hot pressed at higher temperatures. This tenacity is also shown by Rossi and Fulrath's estimate of a monolayer of  $\text{H}_2\text{O}$  still covering 15% of the surface of A  $\text{Al}_2\text{O}_3$  at 1250°C (with only 2 to 5% needed to inhibit final densification). Second is the fact that other gaseous impurities or gas-producing species are present which may not be affected by their treatment. Third is the fact that the authors' use of isopropyl alcohol in milling MgO additions (but no vacuum drying) had no significant effect, nor did Fryer (6) observe benefits from first treating the powder with isopropyl alcohol and then vacuum outgassing at 350°C. However, Fryer's application of pressure earlier in the hot-pressing cycle (at 350°C) may have trapped gases that would have come off before Rossi and Fulrath's application at 800°C. Also, such a treatment may not be applicable to gamma and delta aluminas, since they may contain  $\text{H}_2\text{O}$  in the lattice (to temperatures of at least 1100 to 1200°C) (22). On the other hand, Rossi and Fulrath's time of 300 minutes to achieve about 98% of theoretical density at 1200°C with 5000 psi is substantially shorter than expected from the present work. Variations with different lots and some effect of earlier application of pressure would appear to explain only part of this difference, so their treatment may warrant further investigation.

The present results and the above discussion clearly show that the relationship between outgassing and the application of pressure must be an important consideration in hot pressing. However, as results with the B, and especially BM,  $\text{Al}_2\text{O}_3$  show, finer

powders often start to shrink away from the die at relatively low temperatures so some compromises may be necessary with such materials. (The fact that inhomogeneities occurred in bodies that did shrink away from the die as well as in those that did not clearly shows that they are not due to die-wall friction.)

The latter two powders clearly show that the approach to final densification can be quite inhomogeneous. The effect of gaseous impurities on final densification is indicated by (a) the greatest inhomogeneity being in powders (B and BM) with the greatest content of gaseous impurities which appear to be inhomogeneously distributed and (b) the occurrence of the densest areas in the interior of the body where temperatures are lower (at least initially) and greater retention of such impurities is expected. Gases trapped in more porous areas (e.g., pressing laminations) would tend to inhibit densification in that area, which, if not initially of a laminar lenticular shape, would become so under pressure. Some of the gaseous impurities might be stabilized as nondecomposing liquids (under pressure) which could lead to liquid-phase sintering as may be the case in MgO (11) and CaO (10), where final densification has often been seen to begin internally. Even without this, the expected  $\text{Al}_2\text{S}_3$  should be a liquid above  $1100^\circ\text{C}$  (14) and might lead to some liquid-phase sintering. Any area with a liquid phase would also take on a lenticular or laminar shape under pressure, so either would be consistent with the observed lenticular and laminar inhomogeneities. The lack of explosion in pressing  $\text{Al}_2\text{O}_3$ , in contrast to their occurrence in MgO (11) and CaO (10), is probably due more to the slower densification of  $\text{Al}_2\text{O}_3$  and possibly a slower rate of release of gaseous impurities.

Recently, Gazza et al (23) observed that the time-temperature data presented in this report were similar to the final densification parameters for their hot pressing of another gamma  $\text{Al}_2\text{O}_3$ . The present work, as well as comparison with Gazza et al (23), shows that if there is any enhanced densification due to pressing through the gamma-alpha transition, it is relatively small or very sensitive to pressing parameters.

**With LiF** — Densification is clearly enhanced with LiF, especially in hot pressing. While the mechanisms cannot be explicitly identified from the present work, it is observed that enhanced interparticle sliding and liquid-phase sintering are probably involved. First, the lack of easy plastic flow in  $\text{Al}_2\text{O}_3$  indicates that the observed limited extrusion must be primarily due to enhanced grain boundary sliding. Second, pressing is above the melting point of LiF, so a liquid phase would be present and  $\text{Al}_2\text{O}_3$  is clearly soluble in cryolite ( $\text{AlF}_3 \cdot 3\text{NaF}$ ) and related fluoride melts that may result from any LiF- $\text{Al}_2\text{O}_3$  reaction. Kainarskii et al (24) have, for example, noted that the addition of 2%  $\text{AlF}_3$  to  $\text{Al}_2\text{O}_3$  powders used for welding  $\text{Al}_2\text{O}_3$  bodies together by hot pressing lowered the temperature needed by 200 to  $300^\circ\text{C}$  (from  $1500^\circ\text{C}$ ).

### Characterization

**Impurities** — The gray and black discoloration, both homogeneous and inhomogeneous, though only occasionally reported (15,25), is known to have been observed in a number of investigations and is thus not unique to the author's experimental procedure. This coloring has often been casually assumed to be due to slight carbon contamination. However, while this may be the cause of some of this discoloration, it does not appear to be consistent with much of the observed discoloration. Specifically, black coloration from carbon contamination should be less at lower temperatures rather than greater, as observed, and it should be least at the center of the body rather than greatest. It is also difficult to understand the green and orange colors observed in the bodies on the basis of carbon contamination.

On the other hand, the observed discoloration could arise from the retention of anion impurities, such as  $\text{OH}^-$ ,  $\text{CO}_3^{--}$ ,  $\text{SO}_4^{--}$ , since greater quantities of these or reductions



of them (e.g.,  $S^{--}$ ) should remain in the center of the body and with the lower temperature hot pressing. Various degrees of solution, precipitation, and reduction could well cause the observed variety of colors. Recently, for example, orange discoloration has been reported in translucent hot-pressed  $MgAl_2O_4$  due to reduction of S impurities to colloidal S (26) corroborating the previously discussed reduction of S compounds in hot pressing. (The author has also observed similar black cores as well as more and larger black spots in dense hot-pressed  $MgAl_2O_4$  bodies.) The greater occurrence of such discoloration in B powders with more gaseous impurities from lower calcining also supports this.

Some of these powders are listed as having only 200 to 300 ppm impurities. However, this is based on only cation analysis and thus shows the dangers in only having incomplete analyses. Further, since the evolution of  $CO_2$  from hot-pressed bodies may well be simply due to retention of part of this contaminant from the powder, detection of carbon in spark-source mass spectrometry is not conclusive proof of carbon contamination from graphite dies.

That an observable amount of such gaseous impurities can be retained from the starting powders is not surprising when one considers the tenacity of the last monomolecular layer of such impurities (5,10,13,14), the rapid, relatively low-temperature densification, and the difficulty of diffusing released gases out of such fine powders (10,11,14). Both atmospheric contamination and its tenacity are shown by Scott's (27) observation of bubbles in sapphire bicrystals welded together by vacuum hot-pressing two single crystals together. The bubbles are located on remnants of fine polishing scratches, pits, and depressions and contain gas that was adsorbed on the surfaces of the crystals despite heating in vacuum to  $1500^\circ C$  prior to pressing. This is corroborated by McRae's (28) observation of  $H_2O$  and  $CO_2$  and related species (e.g.,  $H_2$  and  $CO$ ) being given off in vacuum annealing of both single and polycrystalline  $Al_2O_3$  to temperatures over  $1400^\circ C$ . It is also supported by the difficulty of wearing away such films by friction in vacuum (29).

While the finer powders (from lower temperature calcining) retain much higher quantities of at least some of these impurities (e.g., see Table 3 and Refs. 3 and 8), they do not retain proportionately as much in the hot-pressed state. This is probably due to the conversion to alpha  $Al_2O_3$  with its lower absorption of foreign materials (30) and grain growth during hot pressing (since resultant grain sizes are about the same).

The varied weight changes with firing suggest that a number of changes may occur at different temperatures. The general similarity between these curves (Fig. 12) for the different aluminas suggests that these variations are real. The fact that changes to temperatures of at least  $1800^\circ C$  is corroborated by mass spectroscopic analysis and observed bloating in some bodies that had dark black cores. The cause of this bloating only at these high temperatures cannot be completely determined from the present data. However, the demonstrated presence of S, possibly in the form of  $Al_2S_3$ , suggests this is at least part of the cause, since S does not volatilize significantly until temperatures are over  $1550^\circ C$  (16).

**Microstructure** — The addition of LiF clearly results in exaggerated grain growth, but it cannot be determined whether this is due directly to the LiF or to the reaction of either Li or F with the  $Al_2O_3$ . The inhomogeneous nature of such growth suggests that some critical concentration or some other impurity is necessary for such growth.

The greater occurrence of laminar bands of different grain structure in B and BM  $Al_2O_3$  which showed translucent bands of the same orientation suggests that these are related. This would be expected since less porous (e.g., translucent areas) should have faster grain growth. Gaseous impurities could also be a factor in such a relationship, since grain growth would be inhibited by trapped gases and either inhibited or, more likely, accelerated by liquid phases. The change in grain growth in the  $1400$  to  $1600^\circ C$

range may also be due to changes in these impurities, since this appears to approximately correlate with a change in weight. The occurrence of the extremely exaggerated grain growth of Fig. 16 in some black core areas and the possible relation of these cores to gaseous impurities also suggest that the exaggerated grain growth might be due to such impurities. One possibility is that a critical concentration of  $\text{Al}_2\text{S}_3$  causes excessive grain growth. Thus, on heating to temperatures of 1700 to 1800°C, such a concentration could occur somewhere on the inside of the body as the impurity is volatilized from the surface areas with resultant outward migration. The possible effect of gaseous impurities on exaggerated grain growth is also shown by its generally occurring at lower temperatures in B  $\text{Al}_2\text{O}_3$  and higher temperatures at which the grain growth of B  $\text{Al}_2\text{O}_3$  changes slope. King's (31) observation of idiomorphic grain growth only in specimens hot pressed at lower temperatures, where more gaseous impurities would be retained also, could be due to such impurities. His observation of a faster etching of grain boundaries also may well be due to such impurities at the boundaries rather than residual stress.

The lower rate of grain growth of specimens fabricated at higher temperatures (A' of Fig. 13) is probably primarily due to approaching an equilibrium grain size at a given hot-pressing temperature so that a somewhat higher annealing temperature is needed for further substantial grain growth. The scatter of A' specimens is believed due mainly to porosity effects. King (31) also observed that higher annealing temperatures were needed for grain growth in specimens hot-pressed at higher temperatures.

Smoother areas of fracture (7) suggest cleavage of grains of limited misorientation. This could result from local texturing as a result of limited press forging (32) due to shrinkage of the powder compact away from the die prior to application of pressure. Such forging and local orientation could be enhanced by gaseous impurities aiding grain boundary sliding, since this appears to be important in forging  $\text{Al}_2\text{O}_3$  (32b and 32c).

Pears and Starrett (25), in addition to also observing\* discoloration of dense Linde A  $\text{Al}_2\text{O}_3$ , likewise observed many similar microstructural variations. These variations included (a) typical grain-size variations of one- to three-fold, (b) inhomogeneous exaggerated grains of up to 25 to 50 times the surrounding grains, (c) banding of some of these grain-size variations, (d) oriented, lenticular patches of exaggerated grains, (e) flat featureless areas of fracture, and (f) patches of fine pores, clustered on a grain boundary, or scattered over regions of many grains (but still at grain boundaries) in regions of fine grains. The greater extremes of some of these variations are reasonable in view of the much larger size (12 in. by 12 in. by 1-1/8 in.) hot-pressed bodies supplied to them, since this larger size would have longer heating times, greater thermal gradients, and retain more gaseous impurities to accentuate these variations.

While lower temperature annealing may remove much of the damage from sanded surface, some remnants of the damage remain to relatively high annealing temperatures in contrast to the much easier annealing observed in  $\text{MgO}$  (13) and  $\text{CaO}$  (10).

## SUMMARY AND CONCLUSIONS

The addition of LiF to  $\text{Al}_2\text{O}_3$  significantly enhances densification during hot pressing: e.g., dense bodies can be pressed at temperatures of the order of 1100°C with 5000 psi for 15 to 30 minutes from either gamma or alpha  $\text{Al}_2\text{O}_3$  with 2-w/o LiF. Such bodies also show considerable formability at low strain rates. However, while the additive or products thereof are reduced in both hot pressing and annealing, measurable qualities

\*Actual observations made by Capt. L. L. Fehrenbacher.

remain, which could, for example, be detrimental to high-temperature strengths. The additive leads to exaggerated grain growth during hot pressing, which limits strengths (7). Another important limitation is the retention of gaseous impurities which result in variable increases in porosity on limited annealing.

Hot pressing of gamma and alpha  $\text{Al}_2\text{O}_3$  without LiF requires temperatures a few hundred degrees higher, with no significant difference between the two aluminas. Temperature, time, and pressure are clearly shown to be interchangeable. Some translucent specimens were obtained, indicating that if any end-point density exists, it is very close to theoretical density. Though hot pressing in vacuum and delaying the application of pressure as long as possible (without allowing excessive shrinkage away from the die) appeared to limit the effects of gaseous impurities, some were still retained, generally inhomogeneously, in small, variable quantities in the resultant bodies. They may be a major factor in the powder variations observed and may also cause inhomogeneities in final densification and resultant microstructures.

Mass spectroscopic analysis showed  $\text{H}_2\text{O}$ ,  $\text{CO}_2$ , and  $\text{H}_2\text{S}$  were often given off to variable temperatures, sometimes to near the melting point, indicating considerable tenacity. This is corroborated by weight-loss data, which suggests that a series of changes may occur. Much, and possibly all, of these impurities are due to contamination of the starting powders. They result in some generation of porosity, can lead to high-temperature bloating, and apparently affect grain growth. They are also probably an important factor in mechanical properties indirectly, by affecting microstructure, and directly, by reducing intergranular bonding (7).

Clearly, variable quantities of gaseous impurities are trapped in hot pressing  $\text{Al}_2\text{O}_3$ . While many of their effects are speculative, some are beyond doubt. Since their contents have not been analyzed, or even recognized in most previous work, care is required in using such data, and more work is needed on their effects, especially on mechanical properties. More important, however, is the reduction of such impurities. Since they come mostly from the powders rather than the dies or pressing environment, improved treatment or, more likely, preparation and handling of such powders are needed.

While various problems in hot pressing, especially in the reproducibility and homogeneity of resulting bodies, particularly at the finest grain sizes, have been studied and emphasized, hot pressing is, nevertheless, still a very useful process. Identification of the problems and their probable or known causes should lead to further improvement. Use of the present techniques and materials has given dense specimens with fine grain sizes which have, for example, shown strengths as high as 125,000 to 150,000, 100,000 to 115,000, and 55,000 to 65,000 psi at  $-196^\circ$ ,  $22^\circ$ , and  $1315^\circ\text{C}$ , respectively (7), indicating that further improvement could be quite rewarding.

#### ACKNOWLEDGMENTS

The author acknowledges A. Donovan for fabrication, cutting, grinding, and measuring specimens, as well as for weight and density measurements, A. Jenkins and G. Way for ceramographic work, C. Smith for electron microscopy, R. Racus for electron probe analysis, I. Brower for x-ray analysis, and H. Goldberg for mass spectrometer analysis.

## REFERENCES

1. Spriggs, R.M., and Vasilos, T., "Effect of Grain Size on Transverse Bend Strength of Alumina and Magnesia," *J. Am. Ceram. Soc.* 46(No. 5):224-28 (1963)
2. Spriggs, R.M., Mitchell, J.B., and Vasilos, T., "Mechanical Properties of Pure, Dense Aluminum Oxide as a Function of Temperature and Grain Size," *J. Am. Ceram. Soc.* 47(No. 7):323-27 (1964)
3. Passmore, E.M., Spriggs, R.M., and Vasilos, T., "Strength-Grain Size-Porosity Relations in Alumina," *J. Am. Ceram. Soc.* 48(No. 1):1-7 (1965)
4. Vasilos, T., and Spriggs, R.M., "Pressure Sintering: Mechanisms and Microstructures for Alumina and Magnesia," *J. Am. Ceram. Soc.* 46(No. 10):493-96 (1963)
5. Rossi, R.C., and Fulrath, R.M., "Final Stage Densification in Vacuum Hot-Pressing of Alumina," *J. Am. Ceram. Soc.* 48(No. 11):558-64 (1965)
6. Fryer, G.M., "Hot Pressing of Alumina, A New Treatment of Final Densification," *Trans. Brit. Ceram. Soc.* 66(No. 3):127-134 (1967)
7. Rice, R.W., "Strength and Fracture of Dense  $\text{Al}_2\text{O}_3$ ," to be published
8. Henry, J.L., and Kelly, H.J., "Preparation and Properties of Ultrafine High-Purity Alumina," *J. Am. Ceram. Soc.* 48(No. 4):217-18 (1965)
9. Royce, P.V., Jr., Reynolds Metal Company, private communication
10. Rice, R.W., "CaO: I — Fabrication and Characterization," accepted for publication in *J. Am. Ceram. Soc.*
11. Rice, R.W., "Fabrication of Dense MgO," submitted for publication
12. Lang, S.M., "Properties of High-Temperature Ceramics and Cermets — Elasticity and Density at Room Temperature," National Bureau of Standards Monograph 6, Mar. 1960
13. Rice, R.W., "Characterization of Hot Pressed MgO," submitted for publication
14. Rice, R.W., "The Effect of Gaseous Impurities on the Hot Pressing and Behaviour of MgO, CaO, and  $\text{Al}_2\text{O}_3$ ," *Proc. Brit. Ceram. Soc. No. 12: Fabrication Science*, pp. 99-123, Mar. 1969
15. Sellers, D., and Niesse, J.E., "The Development of Hot Pressed Alumina for Gas Bearing Applications," AVCO Corporation, Final Report for Contract N00030-66-C-0189, sub-contract 362, Feb. 1969
16. Handbook of Chemistry and Physics, 37th ed., (Chemical Rubber Pub. Co.)
17. Jones, W.M., and Evans, R.E., "Adsorption of  $\text{CO}_2$  at High Pressures (1-100 atm) by Alumina, Determined from Measurement of Dielectric Constant," *Trans. Faraday Soc.* V62:1596-1607 (1966)
18. Mangsen, G.E., Lambertson, W.A., and Best, B., "Hot Pressing of Aluminum Oxide," *J. Am. Ceram. Soc.* 43(No. 2):55-59 (1960)
19. Mackenzie, J.K., and Shuttleworth, R., "A Phenomenological Theory of Sintering," *Proc. Phys. Soc. (London)* B62:833-852 (1949)

20. Crandall, W.B., Chang, D.H., and Gray, T.J., "The Mechanical Properties of Ultra-Fine Hot-Pressed Alumina," pp. 349-376 in *Mechanical Properties of Engineering Ceramics* (W. Krieger and H. Palmour III, eds.), New York: Interscience, 1961
21. Gardner, W.J., McClelland, J.D., and Richardson, J.H., "Translucent Oxides," Aerospace Corp., Laboratories Div., Report TDR-269(4240-G1)-1 for Contract AF 04(695)-269, Sept. 13, 1963
22. Yanagida, H., Yamaguchi, G., and Kubota, J., "Two Types of Water Contained in Transient Aluminas," *Bull Chem Soc. Japan* 38(No. 12):2194-96 (1965)
23. Gazza, G.E., Barfield, J.R., and Press, D.L., "Reactive Hot Pressing of Alumina with Additives," *Am. Ceram. Soc. Bull.* 48(No. 6):606-10 (1969)
24. Kainarskii, I.S., Oegtyareva, E.V., and Boyarina, I.L., "Diffusion Welding of Corundum Pieces," *Soviet Refractories*, (Trans. from *Ogneupory*, No. 10, pp. 35-40, Oct. 1968) pp. 643-47, 1968
25. Pears, C.D., and Starrett, H.S., "An Experimental Study of the Weibull Volume Theory," Southern Research Institute Technical Report AFML-TR-66-228, Mar. 1967
26. Palmour, H., III (North Carolina State University), discussion in the Hot Forming Symposium, 71st Annual Meeting, American Ceramic Society, Washington, D.C. May 1969
27. (a) Scott, W.D., "Behavior of Pores Located in Grain Boundaries in Pressure-Sintered Aluminum Oxide Bicrystals," presented at 68th Annual Meeting of the American Ceramic Society, Washington, D.C. 1966 (Abstract: *Am. Ceram. Soc. Bull.* 45(No. 4):363 (1966))  
  
(b) Scott, W.D., "Porosity Distribution and Pore Growth in Grain Boundaries of  $\text{Al}_2\text{O}_3$  Bicrystals," to be published
28. McRae, R.C., "Outgassing of  $\text{Al}_2\text{O}_3$  and BeO in Vacuum at 540° and 870°C," presented at the Pacific Coast Meeting, American Ceramic Society, San Francisco, Calif., Nov. 1-3, 1967 (Abstract: *Am. Ceram. Bull.* 46(No. 9):894 (1967))
29. Bowden, F.P., and Hamwell, A.E., "The Friction of Clean Crystal Surfaces," *Proc. Roy. Soc. A* 295(No. 1442):233-43 (1966)
30. Ryshkewitch, E., *Oxide Ceramics*, New York: Academic Press, pp. 116-118, 1960
31. King, A.G., "The Influence of Microstructure on the Mechanical Properties of Dense Polycrystalline Alumina," *Mechanical Properties of Engineering Ceramics* (ed. by W. Krieger and H. Palmour III), New York: Interscience, pp. 333-45, 1961
32. (a) Rhodes, W.H., Sellers, D.J., Vasilos, T., Heuer, A.H., Duff, R., and Burnett, P., "Microstructure Studies of Polycrystalline Refractory Oxides," Avco Corp., Space Systems Div., Summary Report for Contract NOW-65-0316-f (1966)  
  
(b) Rice, R.W., "Hot Working of Refractory Oxides," in *Refractory Oxides* (A. Alper, editor), in publication by Academic Press  
  
(c) Rice, R.W., "Hot Forming of Ceramics," in *Ultrafine Grain Ceramics* (ed. by Burke, et al), in publication by Syracuse University Press

## DOCUMENT CONTROL DATA - R &amp; D

Security classification of title, body of abstract and indexing annotation must be entered when the overall report is classified

1 ORIGINATING ACTIVITY (Corporate author)		2a. REPORT SECURITY CLASSIFICATION	
Naval Research Laboratory Washington, D.C. 20390		Unclassified	
3 REPORT TITLE		2b. GROUP	
FABRICATION AND CHARACTERIZATION OF HOT PRESSED $Al_2O_3$			
4 DESCRIPTIVE NOTES (Type of report and inclusive dates)			
An interim report on the problem; work is continuing.			
5 AUTHOR(S) (First name, middle initial, last name)			
Roy W. Rice			
6 REPORT DATE	7a. TOTAL NO OF PAGES	7b. NO OF REFS	
July 7, 1970	30	32	
8a. CONTRACT OR GRANT NO	9a. ORIGINATOR'S REPORT NUMBER(S)		
NRL Problem C 05-28	NRL Report 7111		
b. PROJECT NO	9b. OTHER REPORT NO(S) (Any other numbers that may be assigned this report)		
Project RR 007-02-41-5677			
c.			
d.			
10 DISTRIBUTION STATEMENT			
This document has been approved for public release and sale; its distribution is unlimited.			
11 SUPPLEMENTARY NOTES		12 SPONSORING MILITARY ACTIVITY	
		Department of the Navy (Office of Naval Research), Arlington, Va. 22217	
13 ABSTRACT			
<p>Hot pressing of <math>Al_2O_3</math> with and without LiF is described, and the resultant bodies are characterized. Addition of LiF significantly enhances densification, allowing dense bodies to be obtained at about <math>1100^\circ C</math>, which is 200 to <math>300^\circ C</math> lower than without additives. However, the additives result in exaggerated grain growth even during hot pressing. Though the fluoride content is reduced, both during hot pressing and subsequent annealing, some fluoride remains which could be detrimental to some properties of bodies made with LiF. Some of the problems and defects of pressing are emphasized as an aid to improving the process. Particular attention is given to the analysis of <math>H_2O</math>, <math>CO_2</math>, and S impurities (which are probably present as chemically bonded anions) and some of their known and possible effects on microstructure and behavior in materials made with and without additives.</p>			

KEY WORDS	LINK A		LINK B		LINK C	
	ROLE	KT	ROLE	WT	ROLE	WT
Hot pressing Al <sub>2</sub> O <sub>3</sub> LiF Microstructure Ceramics Characterization Impurities Grain growth						